Supplement of Atmos. Meas. Tech., 17, 2761–2776, 2024
https://doi.org/10.5194/amt-17-2761-2024-supplement

Atmospheric Measurement Techniques
Open Access
EGU

Supplement of

Characterization of the airborne aerosol inlet and transport system used during the A-LIFE aircraft field experiment

Manuel Schöberl et al.

Correspondence to: Bernadett Weinzierl (bernadett.weinzierl@univie.ac.at)

S1 A-LIFE in-cabin instrumentation

As can be seen in Fig. 1 in the main manuscript, the aerosol particles enter the isokinetic inlet tube after passing a diffuser and a 90° bend. The isokinetic inlet tube is the only part in the sampling system through which the volumetric flow of the entire in-cabin instrumentation passes. It has an inner diameter of 4.572 mm and is approximately 35 cm long (see red line, solid and dashed, in the inlet sketch in Fig. S1). To estimate the flow regime in the isokinetic inlet tube, we calculated the flow Reynolds number for the minimum and maximum flow of the A-LIFE in-cabin instrumentation (17.87 L min^{-1} and 22.83 L min^{-1} or 18.14 m s^{-1} and 23.18 m s^{-1}, respectively). The air density and viscosity were calculated with averaged values of temperature and pressure over the investigated v_{TAS} range. Figure S1 displays the flow Reynolds number as a function of true airspeed v_{TAS}. The values for minimum and maximum flows are always larger than 2000. Therefore, it can be concluded that the flow conditions in the isokinetic inlet tube were never laminar during the A-LIFE field campaign.

Table S1 lists aerosol instruments that were installed in the aircraft cabin of the *Falcon* and were connected to the isokinetic inlet during the A-LIFE mission. The instrument setup including the flows in the different sampling line parts can be seen in Fig. S2. Two experimental instruments which drew together 2.85 L min^{-1} are not included in Table S1 and Fig. S2.

As mentioned above, the A-LIFE instrumentation drew in total a volumetric flow of a minimum of 17.87 L min^{-1} which could increase to a maximum of 22.83 L min^{-1}. The value of the total flow varies because two impactor devices were only turned on during selected measurement periods (typically six times for 5-10 minutes per flight) which increased the total flow by 0.96 L min^{-1} (Kandler et al., 2007) during these periods. Furthermore, the so-called constant pressure inlet (CPI) system of the DMT Cloud Condensation Nuclei Counter (CCNC) caused a varying flow depending on altitude. The inlet system of the CCNC was used to ensure measurements at a fixed pressure of 500 hPa. The CPI system consists of two orifices with different diameters used at different altitudes, and a pump. Depending on the ambient pressure, the pump regulated the flow (between 0 and 4 L min^{-1}) so that a pressure of 500 hPa was established behind the orifice.

S2 Aerosol number size distribution

For the derivation of the aerosol number size distribution (NSD) for each of the 262 A-LIFE flight sequences, the data of four instruments were used. The instruments and their nominal size ranges, as well as the size ranges used for the combined NSDs, are summarized in Table S2.

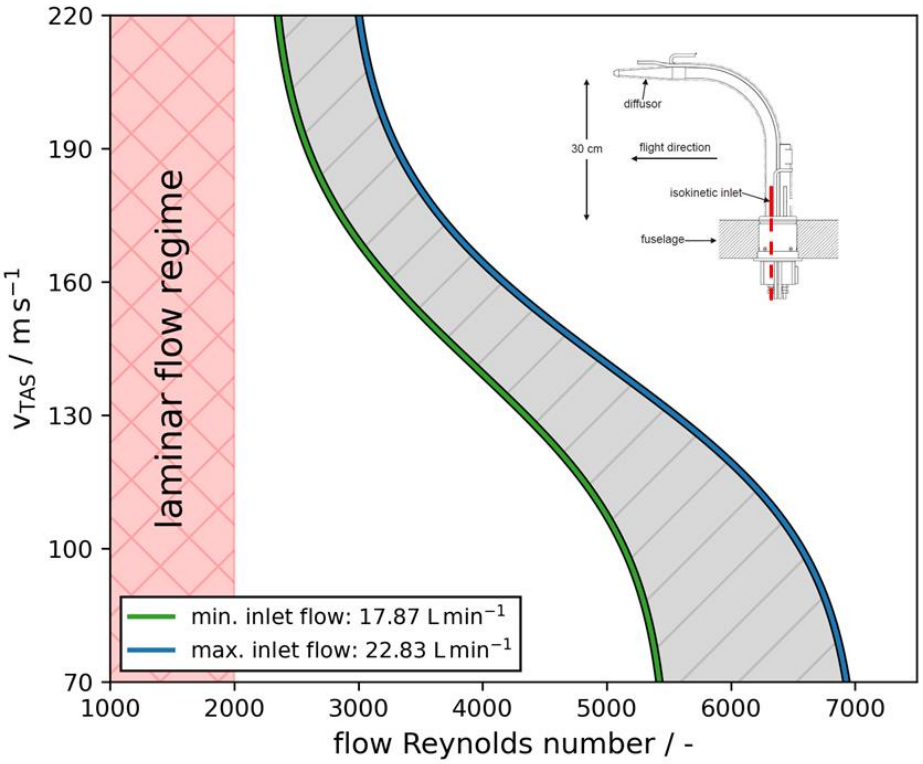

Figure S1: Flow Reynolds number (flow Re) as a function of v_{TAS} for the 35 cm long isokinetic inlet tube. The isokinetic inlet tube is marked with red lines in the upper right corner of the plot (solid line for the part outside the aircraft's fuselage, dashed for the part inside). The red hatch area marks the region where laminar flow conditions would be established (flow Re < 2000). For the calculation of flow Re averaged values of ambient pressure and temperature as a function of v_{TAS} were used for the calculation of the air density and viscosity.

Table S1: Overview of the in-cabin instrumentation which was connected to the isokinetic inlet during A-LIFE.

Instrument	Manufacturer	Nominal flow [L min^{-1}]	Tubing length [m]	Measured quantity
CPC1	TSI	1	5.83	Integral particle number concentration
CPC2	TSI	1.5	2.66	Integral particle number concentration
CPSA1	Custom-built at DLR	1	2.39	Integral non-volatile particle number concentration
CPSA2	Custom-built at DLR	1	2.47	Integral non-volatile particle number concentration
CPSA3	Custom-built at DLR	1	2.22	Integral particle number concentration
SkyOPC	Grimm	1.2	1.52	Aerosol number size distribution
SkyOPCTD	Grimm	1.2	3.49	Non-volatile aerosol number size distribution
Impactor device 1	Custom-built at TU Darmstadt	0.48	0.92	Chemical particle composition, shape
Impactor device 2	Custom-built at TU Darmstadt	0.48	1.02	Chemical particle composition, shape
SP2 (+ bypass)	DMT	0.12 (+ 2)	1.59	Refractory black carbon mass
CCNC (+ CPI)	DMT	1 (+ 0-4)	2.85	Number concentration of cloud condensation nuclei at various supersaturations
Aurora 4000 nephelometer	Ecotech	2	2.68	Scattering coefficient at three wavelengths (450, 525 and 635 nm)
TAP	Brechtel	2	3.52	Absorption coefficient at three wavelengths (465, 520 and 640 nm)

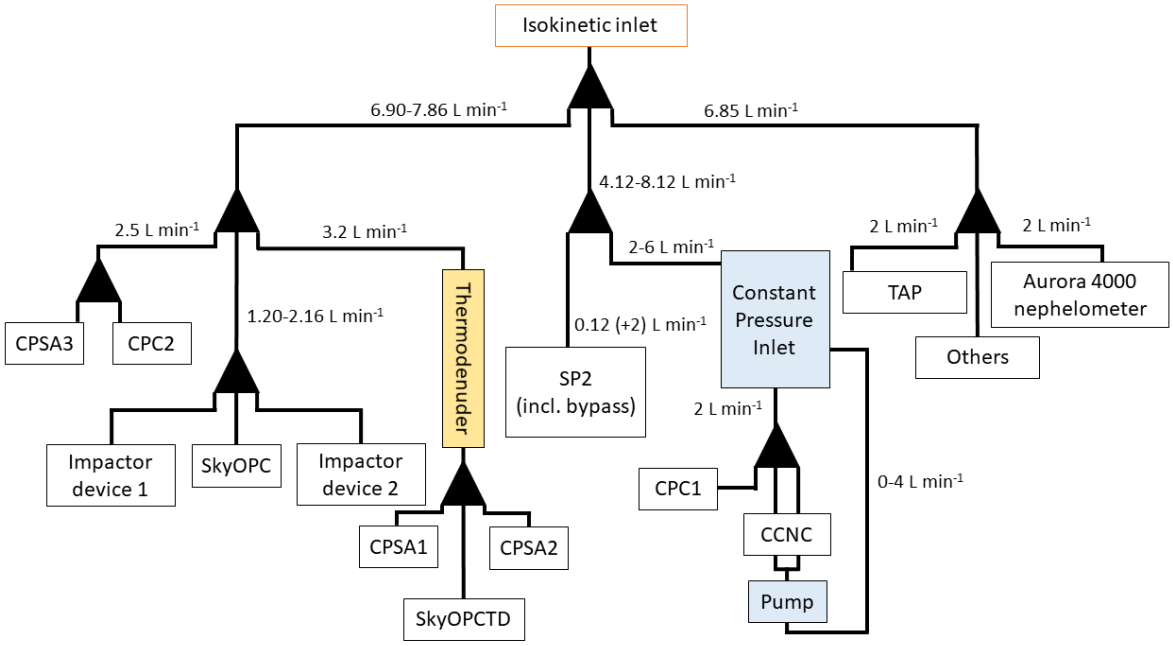

Figure S2: Flow plan of the in-cabin instrumentation that was connected to the isokinetic inlet. Note, this flow plan shows the default setup for the A-LIFE campaign which was flown almost the entire time. However, for testing purposes, it was also possible to operate the SkyOPCTD without thermodenuder or behind the constant pressure inlet.

Table S2: Instrumentation used for the derivation of the aerosol number size distribution (NSD) for each of the 262 A-LIFE flight sequences. Each instrument was set to a time resolution of 1 Hz.

Instrument type	Instrument model	Nominal size range	Size range used for combined NSD	Location
Condensation particle counter	TSI3760a (CPC2)	10 nm < D_p	10 nm < D_p	In-cabin (particles measured at dry conditions)
Optical particle counter	Grimm SkyOPC 1.129 (SkyOPC)	250 nm < D_p < 3 µm	280 nm < D_p < 3 µm (for in-cabin NSD) 280 nm < D_p < 1 µm (for full-size-range NSD)	In-cabin (particles measured at dry conditions)
Optical particle counter	DMT Ultra High Sensitivity Aerosol Spectrometer Airborne (UHSAS-A)	60 nm < D_p < 1000 nm	125 nm < D_p < 400 nm	Mounted under the aircraft wing (actively-pumped and dried sample flow)
Optical particle counter	DMT Cloud and Aerosol Spectrometer (UNIVIE CAS – optical spectrometer part of the UNIVIE CAPS)	0.5 < D_p < 50 µm	0.9 µm < D_p < 50 µm (for full-size-range NSD only)	Mounted under the aircraft wing (passive flow; particles measured at ambient relative humidity conditions)

S3 Transport efficiency

In this study, the transport efficiency was calculated with empirical equations from literature. For Fig. 8 in the main manuscript, the inlet efficiency was derived with the experimentally determined sampling efficiency (inlet + transport efficiency) and the calculated transport efficiency. For this, the transport efficiency of the SkyOPC was used. The transport system for the SkyOPC is summarized in Table S3. The volumetric flow, the length as well as the bend angles were used for the calculation of the efficiency of each tubing part. For the first four sampling line pieces the mean of the flow range was used. The inner diameter of all 9 tubing parts is 4.572 mm.

For the losses of coarse-mode aerosol particles in the tubing system, two loss mechanisms were considered: losses in tubing bends and sedimentation losses. For all calculations, the aerosol particle itself was assumed to be a mineral dust particle (density ρ = 2.6 g cm^{-3} and dynamic shape factor χ = 1.2; Hess et al., 1998 and Kaaden et al., 2009).

S3.1 Particle losses in bends

For aerosol particle losses in bends of sampling lines, the following equation given by Pui et al., 1987 was used:

$$\eta_{\mathrm{bend}} = \left(1 + \left(\frac{\mathrm{Stk}}{0.171}\right)^{0.452\frac{\mathrm{Stk}}{0.171}+2.242}\right)^{-\frac{2}{\pi}\theta} \quad \text{(S1)}$$

Here, θ is the angle of curvature of the sampling line in degrees and Stk represents the Stokes number. For the calculation of the Stokes number, the following equations were used (S2-S5; Seinfeld and Pandis, 2016):

$$\eta = 1.7188 \cdot 10^{-5}\left[\left(\frac{\mathrm{T}}{273.15}\right)^{1.5}\left(\frac{384.15}{\mathrm{T}+111}\right)\right] \quad \text{(S2)}$$

$$\lambda = 0.0651\ \frac{\eta}{1.8\cdot 10^{-5}}\ \frac{1013}{\mathrm{p}}\ \sqrt{\frac{\mathrm{T}}{298}} \quad \text{(S3)}$$

$$\mathrm{C_C} = 1 + \frac{2\lambda}{\mathrm{D_p}}\left[1.257 + 0.4\exp\left(\frac{-1.1\ \mathrm{D_p}}{2\lambda}\right)\right] \quad \text{(S4)}$$

$$\mathrm{Stk} = \frac{\rho\ \mathrm{D_p}^2\ \mathrm{C_c}\left(\frac{\mathrm{v_{TAS}}}{7.1}\right)}{18\ \eta\ \mathrm{D}\ \chi} \quad \text{(S5)}$$

Here, η is the dynamic viscosity of air, λ the mean free path of the ambient air, Cc the Cunningham slip correction factor. p represents the ambient pressure, while T is the temperature inside the aircraft cabin respectively inside the sampling line, which is assumed to be 30°C. D represents the inner diameter of the sampling line.

S3.2 Sedimentation losses

For aerosol particle losses in bends of sampling lines, the following equation given by Thomas (1958) and Fuchs (1964) was used:

$$\eta_{sed} = 1 - \frac{2}{\pi}\left(2\,\epsilon\sqrt{1-\varepsilon^{\frac{2}{3}}} - \varepsilon^{\frac{1}{3}}\sqrt{1-\varepsilon^{\frac{2}{3}}} + \arcsin\sqrt[3]{\epsilon}\right) \quad \text{(S6)}$$

$$\text{with } \epsilon = \frac{3\,L\,v_{TS}}{4\,D\,Q} \cdot \cos\theta \quad \text{(S7)}$$

given by Heyder and Gebhart (1977). Here, θ is the angle of inclination, L the length of the sampling line, Q the volumetric flow, D the inner diameter of the sampling line and v_{TS} the particle terminal settling velocity, which was calculated with the following equation (Seinfeld and Pandis, 2016):

$$v_{TS} = \frac{\rho\,D_p^{\,2}\,C_c\,g}{18\,\eta\,\chi} \quad \text{(S8)}$$

Table S3: Overview of all sampling line pieces which formed the transport system of the SkyOPC.

Sampling line	Flow [L min^{-1}]	Length [m]	Bend angle [°]
#1	6.90-7.86	0.14	80
#2	6.90-7.86	0.12	0
#3	1.20-2.16	0.12	0
#4	1.20-2.16	0.12	0
#5	1.2	0.25	90
#6	1.2	0.30	0
#7	1.2	0.25	90
#8	1.2	0.10	0
#9	1.2	0.12	0

S4 Fitted ambient pressure and temperature

As explained in Sect. 2.4.3 in the main manuscript, we used the Stokes number Stk_{50} of each v_{TAS} value to convert back to a new cutoff diameter $D_{p,50}$. For this, we used fitted values of ambient pressure and temperature for the whole v_{TAS} range from 70 to 220 m s^{-1}. The used sigmoid fits for this approach are displayed in Fig. S3 and Fig. S4.

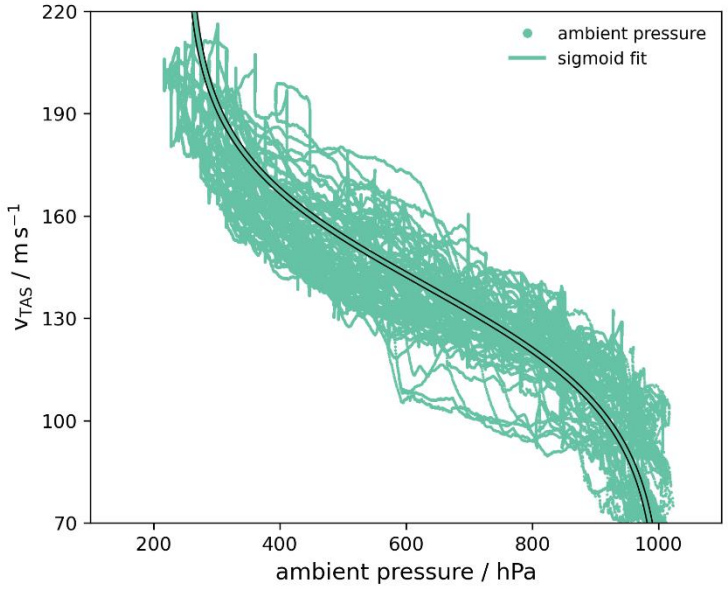

Figure S3: Ambient pressure as a function of v_{TAS}. The points show the 1 s data measured by the CMET system of the *Falcon* during the A-LIFE campaign. The straight line depicts the sigmoid fit which was used for the calculation of the cutoff diameters.

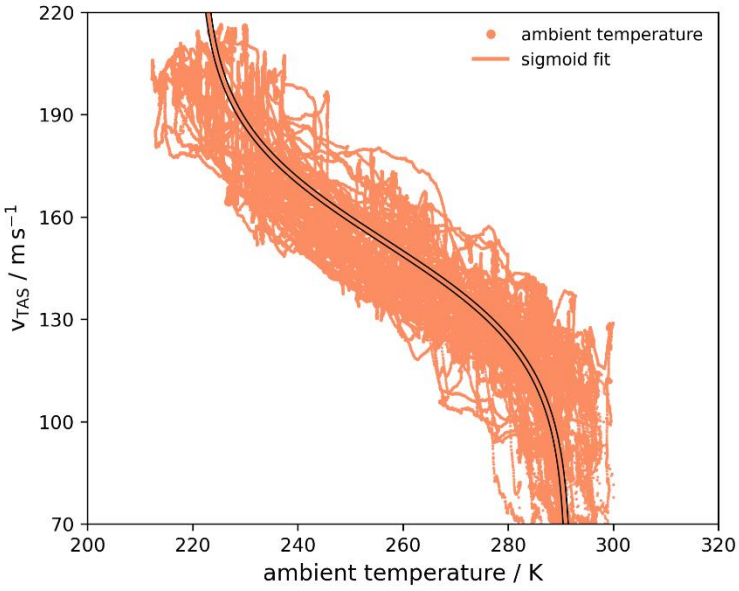

Figure S4: Ambient temperature as a function of v_{TAS}. The points show the 1 s data measured by the CMET system of the *Falcon* during the A-LIFE campaign. The straight line depicts the sigmoid fit which was used for the calculation of the cutoff diameters.

References

Fuchs, N.: The Mechanics of Aerosols, Pergamon, Oxford, https://doi.org/10.1002/qj.49709138822, 1964.

Hess, M., Koepke, P., & Schult, I.: Optical Properties of Aerosols and Clouds: The Software Package OPAC, B. Am. Meteor. Soc., 79, 831–844, doi:10.1175/15200477(1998)079<0831:OPOAAC>2.0.CO;2, 1998.

Heyder, J. and Gebhart, J.: Gravitational deposition of particles from laminar aerosol flow through inclined circular tubes, J. Aerosol Sci., 8, 289–295, https://doi.org/10.1016/0021-8502(77)90048-9, 1977.

Kaaden, N., Massling, A., Schladitz, A., Müller, T., Kandler, K., Schütz, L., Weinzierl, B., Petzold, A., Tesche, M., Leinert, S., Deutscher, C., Ebert, M., Weinbruch, S., and Wiedensohler, A.: State of mixing, shape factor, number size distribution, and hygroscopic growth of the Saharan anthropogenic and mineral dust aerosol at Tinfou, Morocco, Tellus B Chem. Phys. Meteorol., 61, 51–63, https://doi.org/10.1111/j.1600-0889.2008.00388.x, 2009.

Kandler, K., Benker, N., Bundke, U., Cuevas, E., Ebert, M., Knippertz, P., Rodríguez, S., Schütz, L., and Weinbruch, S.: Chemical composition and complex refractive index of Saharan Mineral Dust at Izaña, Tenerife (Spain) derived by electron microscopy, Atmos. Environ., 41, 8058–8074, https://doi.org/10.1016/j.atmosenv.2007.06.047, 2007.

Pui, D. Y. H., Romay-Novas, F., and Liu, B. Y. H.: Experimental Study of Particle Deposition in Bends of Circular Cross Section, Aerosol Sci. Technol., 7, 301–315, https://doi.org/10.1080/02786828708959166, 1987.

Seinfeld, J. H. and Pandis, S. N.: Atmospheric chemistry and physics: from air pollution to climate change, John Wiley & Sons, Hoboken, USA, 1326 pp., ISBN: 978-1-118-94740-1, 2016.

Thomas, J. W.: Gravity Settling of Particles in a Horizontal Tube, J. Air Pollut. Control Assoc., 8, 32–34, https://doi.org/10.1080/00966665.1958.10467825, 1958.